Unconventional Majorana fermions on the surface of topological superconductors protected by rotational symmetry

Junyeong Ahn and Bohm-Jung Yang

Phys. Rev. B **103**, 184502 — Published 3 May 2021
DOI: 10.1103/PhysRevB.103.184502

Unconventional Majorana Fermions on the Surface of Topological Superconductors Protected by Rotational Symmetry

Junyeong Ahn[1,2,3,4,5,*] and Bohm-JungYang[1,2,3,†]

[1]Center for Correlated Electron Systems, Institute for Basic Science (IBS), Seoul 08826, Korea
[2]Department of Physics and Astronomy, Seoul National University, Seoul 08826, Korea
[3]Center for Theoretical Physics (CTP), Seoul National University, Seoul 08826, Korea
[4]RIKEN Center for Emergent Matter Science (CEMS), Wako, Saitama 351-0198, Japan
[5]Department of Applied Physics, The University of Tokyo, Bunkyo, Tokyo 113-8656, Japan

(Dated: April 21, 2021)

Topological superconductors are exotic gapped phases of matter hosting Majorana mid-gap states on their boundaries. In conventional three-dimensional topological superconductors, Majorana in-gap states appear in the form of spin-1/2 fermions with a quasi-relativistic dispersion relation. Here, we show that unconventional Majorana states can emerge on the surface of three-dimensional topological superconductors protected by rotational symmetry. The unconventional Majorana surface states are classified into three different categories: a spin-s Majorana fermion with $(2s+1)$-fold degeneracy $(s \geq 3/2)$, a Majorana Fermi line carrying two distinct topological charges, and a quartet of spin-1/2 Majorana fermions related by fourfold rotational symmetry. The spectral properties of the first two types, which go beyond conventional spin-1/2 fermions, are unique to topological superconductors and have no counterparts in topological insulators. We show that unconventional Majorana surface states can be obtained in the superconducting phase of doped Z_2 topological insulators or Dirac semimetals with rotational symmetry.

Topologically stable gapless surface states are the hallmark of three-dimensional (3D) topological insulators (TIs) and topological superconductors (TSCs) [1]. One common feature of such surface states is that they appear as spin-1/2 fermions with a quasi-relativistic dispersion relation. According to the recent classification of TI surface states using wallpaper groups [2], gapless surface states of TIs always have the form of Dirac or Weyl fermions locally, while their global band structure can take various forms [2–4]. However, as crystalline systems do not have Lorentz symmetry, there is no fundamental reason forbidding more exotic dispersion relations. Indeed, the discovery of exotic low-energy excitations in bulk semimetals and bulk nodes of superconductors, such as spin-1 and spin-3/2 fermions [5–9], nodal lines [10–12] and nodal surfaces [13, 14], have shown that unconventional fermionic excitations protected by crystalline symmetries can emerge in bulk crystals. Also, in contrast to TI surface states, symmetry-protected surface Majorana fermions (MFs) of TSCs have not yet been exhaustively characterized. Considering that TSCs have particle-hole symmetry that is absent in TIs, the surfaces of TSCs may host unusual fermions, which go beyond spin-1/2 fermions on TI surfaces.

Here, we show that unconventional MFs emerge on the surfaces of TSCs protected by n-fold rotation C_n and time-reversal T symmetries. By analyzing all possible realizations of anomalous surface states, we find that rotation-protected TSCs feature three types of surface MFs, two of which exhibit characteristic energy spectra that have no counterparts in TIs. The first type takes the form of *higher-spin Majorana fermions* (HSMFs), which generalize the spin-3/2 fermion in semimetals [5–8] when the superconducting pairing function is invariant under C_n (we call this even-C_n pairing) [see Fig. 1(a)]. As higher-spin states cannot be realized on the boundaries of TIs with any wallpaper symmetry groups [2], they are unique to TSCs. Furthermore, the HSMF cannot exist in the bulk of isolated two-dimensional (2D) nodal superconductors because their protection requires an anomalous C_n symmetry representation. On the other hand, when the pairing function changes sign under $C_{n=2,6}$ (we call this odd-$C_{n=2,6}$ pairing), a *doubly charged Majorana Fermi line* (DCMFL), carrying both zero-dimensional (0D) and one-dimensional (1D) topological charges, appears [Fig. 1(b,d)]. While the 0D topological charge indicates the local stability of the DCMFL, the 1D topological charge guarantees its global stability [14]. Finally, when the pairing function changes its sign under C_4 (odd-C_4 pairing), a quartet of Majorana fermions (QMF) with twofold degeneracy appears on a C_4 invariant surface [Fig. 1(c)] This is a superconducting analog of the C_4 rotation anomaly that was recently proposed in TIs protected by C_n and T symmetries [15]. We show that all three types can appear when superconductivity emerges in doped $\mathbb{Z}_2$ TIs or Dirac semimetals with T and C_n symmetries.

To convey the main ideas concisely, we focus on spin-orbit coupled systems below. However, our theory is also applicable to spin-rotation-symmetric and spin-polarized systems, as explained in detail in the Supplemental Material (SM) [16]. Our surface-state classification is consistent with previous bulk classifications [17–20], which shows that we have exhausted all possible anomalous surface states.

Formalism.— We consider the mean-field Hamiltonian for superconductors in the Bogoliubov-de Gennes (BdG) formalism, $\hat{H} = \frac{1}{2}\sum_{\mathbf{k}} \hat{\Psi}^\dagger_{\mathbf{k}} H_{\mathrm{BdG}}(\mathbf{k}) \hat{\Psi}_{\mathbf{k}}$, where

$$H_{\mathrm{BdG}}(\mathbf{k}) = \begin{pmatrix} h(\mathbf{k}) & \Delta(\mathbf{k}) \\ \Delta^\dagger(\mathbf{k}) & -\sigma_y h^t(-\mathbf{k})\sigma_y \end{pmatrix}, \tag{1}$$

and $\hat{\Psi} = (\hat{c}_{\mathbf{k}}, \hat{c}^\dagger_{-\mathbf{k}} i\sigma_y)^t$ is the Nambu spinor in which $\hat{c}_{\mathbf{k}}/\hat{c}^\dagger_{\mathbf{k}}$ are electron annihilation/creation operators. The superscript t denotes the matrix transpose. $h(\mathbf{k})$ is the normal-state

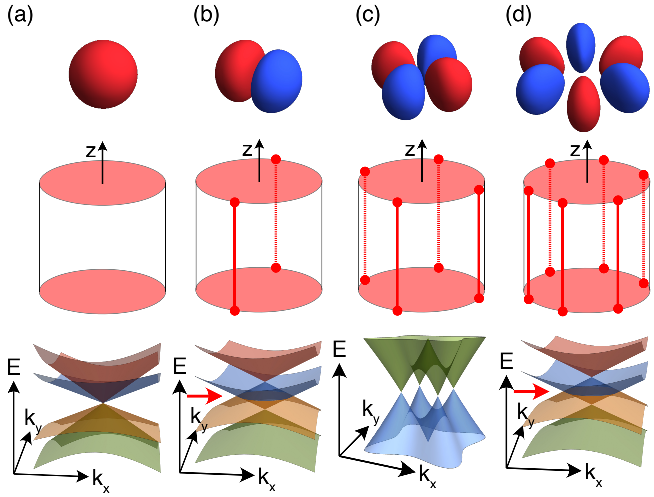

FIG. 1. Majorana boundary states of rotation-protected topological superconductors in 3D. The top panel shows the symmetry of the pairing function under C_n rotation: (a) even-$C_{n=2,3,4,6}$, and (b,c,d) odd-$C_{2,4,6}$. The middle shows the real-space geometry of the system. Here, the z-axis is the rotation axis. Red regions host gapless Majorana fermions. The characteristic surface spectra on C_n-invariant surfaces are shown at the bottom. In (a), only the spectrum with a fourfold degenerate point is shown for clarity, but arbitrary degeneracy can be protected. The red arrow in (b,d) indicates the zero energy where the MFL exists.

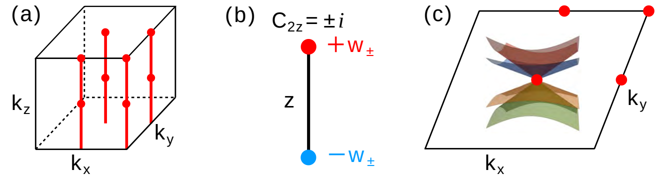

FIG. 2. Bulk topology and surface higher-spin Majorana fermion. (a) C_{2z}-invariant lines in the 3D Brillouin zone, which are located at $(k_x, k_y) = (0,0)$, $(\pi, 0)$, $(0,\pi)$, and (π,π), respectively. (b) The 1D winding number and chirality of edge states in a C_2-invariant line. When the winding numbers $w_\pm$ in the C_2 eigensector with eigenvalues $\pm i$ are nonzero, $|w_\pm|$ Majorana zero modes appear at both edges. The sum of the chirality (the eigenvalue of the chiral operator S) of the zero modes is $+w_\pm$ on one edge and $-w_\pm$ on the other edge. (c). Spin-3/2 fermion appearing at $(k_x, k_y) = (0,0)$ of a C_2-symmetric surface Brillouin zone. Its fourfold degeneracy originates from the nontrivial winding numbers $w_+ = -w_- = \pm 2$ of the line at $(k_x, k_y) = (0,0)$.

Hamiltonian, and the superconducting pairing function $\Delta(\mathbf{k})$ satisfies $\Delta(\mathbf{k}) = -\sigma_y \Delta^t(-\mathbf{k})\sigma_y$ due to the Fermi statistics. This BdG Hamiltonian has particle-hole P symmetry $PH_{\rm BdG}(\mathbf{k})P^{-1} = -H_{\rm BdG}(-\mathbf{k})$ where

$$P = \begin{pmatrix} 0 & -i\sigma_y \\ i\sigma_y & 0 \end{pmatrix} K, \tag{2}$$

which satisfies $P^2 = 1$. We use italic (calligraphic) symbols to indicate the symmetry operator of the BdG Hamiltonian (normal-state Hamiltonian).

Let us assume that the normal state has C_n symmetry about the z-axis, so that $\mathcal{C}_n h(\mathbf{k})\mathcal{C}_n^{-1} = h(R_n\mathbf{k})$, where $R_n\mathbf{k}$ indicates the momentum after $\mathcal{C}_n$ rotation of $\mathbf{k}$. When $\Delta(\mathbf{k})$ is an eigenfunction of C_n, i.e., $\mathcal{C}_n\Delta(\mathbf{k})\mathcal{C}_n^{-1} = \lambda\Delta(R_n\mathbf{k})$, $H_{\rm BdG}$ is symmetric under $C_n \equiv \mathrm{diag}[\mathcal{C}_n, \lambda\mathcal{C}_n]$ which satisfies $C_nP = \lambda PC_n$. Namely, $C_nH_{\rm BdG}(\mathbf{k})C_n^{-1} = H_{\rm BdG}(R_n\mathbf{k})$.

Now we suppose that the normal state has time reversal symmetry $\mathcal{T}h(-\mathbf{k})\mathcal{T}^{-1} = h(\mathbf{k})$, under $\mathcal{T} = i\sigma_y K$. When the pairing function is also time-reversal-symmetric, i.e., $\mathcal{T}\Delta(\mathbf{k})\mathcal{T}^{-1} = \Delta(-\mathbf{k})$, the BdG Hamiltonian is symmetric under $T = \mathrm{diag}(\mathcal{T}, \mathcal{T})$. Consistency with $\mathcal{C}_n$ invariance requires $\lambda = \lambda^*$ for $\mathcal{T}$-preserving pairing, because $\mathcal{T}\mathcal{C}_n = \mathcal{C}_n\mathcal{T}$. Accordingly, $C_nP = \pm PC_n$ in T-symmetric superconductors, such that the pairing is either even-C_n ($\lambda = 1$) or odd-C_n ($\lambda = -1$). For our analysis below, it is convenient to define the chiral symmetry operator $S = iTP$ satisfying $C_nS = \pm SC_n$ and $S^2 = 1$. The commutation relations shown here are generally valid, independent of basis choice.

Higher-spin Majorana fermions (HSMFs).— Let us first consider the surface states of TSCs with even-C_n pairing characterized by the relation $C_nP = PC_n$, focusing on the $n = 2$ case. On a C_2-invariant surface, the simplest form of the surface states is the twofold degenerate MF with a linear dispersion relation, protected by chiral symmetry. More explicitly, when we take the representation $S = \sigma_z$ and $T = i\sigma_y K$ with Pauli matrices $\sigma_{x,y,z}$, a Majorana surface state can be described by the Hamiltonian $H_s(k_x, k_y) = v_xk_x\sigma_x + v_yk_y\sigma_y$, which carries a winding number $w = \mathrm{sgn}(v_xv_y) = \pm1$, where $w = (i/4\pi)\oint_\ell d\mathbf{k}\cdot \mathrm{Tr}\left[SH_s^{-1}\nabla_\mathbf{k}H_s\right]$ is defined along a loop ℓ surrounding the node at $\mathbf{k} = 0$. The total winding number of surface MFs is protected by chiral symmetry, so it is robust independent of C_2 symmetry.

To obtain surface states that require C_2 symmetry for their protection, let us consider a four-band surface Hamiltonian describing two overlapping MFs with opposite winding numbers: $H_s(k_x, k_y) = k_x\sigma_x + k_y\rho_z\sigma_y$, which is invariant under $S = \sigma_z$ and $T = i\sigma_yK$. Then, possible C_2 representations commuting with S and T, and satisfying $(C_2)^2 = -1$, are $C_2 = -i\rho_z\sigma_z$ and $C_2 = -i\sigma_z = -iS$. In the former case, a mass term $m\rho_y\sigma_y$ opens the gap on the surface. On the other hand, in the latter case, no mass term is allowed, so the gapless spectrum is protected. In fact, the fourfold degeneracy at $\mathbf{k} = 0$ is *enforced* by the representation $C_2 = \pm iS$ because

$$H_s(\mathbf{k}) = -SH_s(\mathbf{k})S^{-1} = -C_2H_s(\mathbf{k})C_2^{-1} = -H_s(-\mathbf{k}), \tag{3}$$

so that $H_s(\mathbf{k} = \mathbf{0}) = 0$. This type of symmetry-enforced degeneracy is possible only on the surface of a TSC because $C_2 = \pm iS$ is an anomalous representation that mixes the particle-hole indices, which is impossible in an ordinary C_2 representation of the bulk states.

The fourfold degenerate point disperses like spin-3/2 fermions [5–8] because the degeneracy is lifted away from the C_2-invariant momentum $\mathbf{k} = 0$. In fact, the representation $C_2 = \pm iS$ can generally protect $2n$-fold degenerate points with an arbitrary natural number n, which we call spin-$(2n-1)/2$ MFs (or more generally, HSMFs).

We can understand the corresponding 3D bulk topology of H_{BdG} using the 1D topology on C_2-invariant lines [Fig. 2(a)], as shown in Ref. [20]. From this, the origin of the anomalous representation $C_2 = \pm iS$ on the surface can be found. Let us recall that, in 1D systems with winding number w, w zero modes with positive (negative) chirality appear on one (the other) edge [21, 22] [see Fig. 2(b)]. On C_2-invariant lines, the winding numbers $w_\pm$ can be defined in two distinct sectors with C_2 eigenvalues $\pm i$, respectively. As time reversal symmetry imposes that $w_+ + w_- = 0$ [16], $w_+ = -w_- \in \mathbb{Z}$ is the remaining invariant on a C_2-invariant line, which naturally leads to the anomalous representation $C_2 = \pm iS$ at its edge. This guarantees the protection of degeneracies at the C_2-invariant momentum on the top and bottom surfaces, as shown in Fig. 2(c). As the total winding number is zero, the degeneracy at zero energy is lifted away from the C_2-invariant momentum. Similarly, HSMFs in TSCs with even-$C_{n=3,4,6}$ pairing can be protected by the 1D winding number defined in each C_n eigensector [16].

Doubly charged Majorana Fermi lines (DCMFLs).— Next, we consider odd-C_2 pairing characterized by $C_2S = -SC_2$. Odd-C_6 pairing also falls into this category. In these cases, no HSMF is allowed [16]. Instead, surface states appear at generic momenta. Since $\mathbf{k}$-local symmetries C_2T and C_2P satisfy $(C_2T)^2 = (C_2P)^2 = 1$, gap nodes appear as lines, i.e., Majorana Fermi lines (MFLs), at generic momenta [14].

To understand the anomalous MFL, let us consider a Dirac fermion on a C_2-invariant surface of a TI described by the Hamiltonian $h_D = -\mu + k_x\sigma_x + k_y\sigma_y$ invariant under $\mathcal{C}_2 = -i\sigma_z$ and $\mathcal{T} = i\sigma_y K$. Then, there is a unique odd-C_2 pairing function $\Delta(k_x,k_y) = [\mathbf{\Delta}\cdot\mathbf{k} + O(k^3)]\sigma_z$ that gives the following surface BdG Hamiltonian

$$H_{\mathrm{BdG}}(k_x,k_y) = k_x\tau_z\sigma_x + k_y\tau_z\sigma_y - \mu\tau_z + \mathbf{\Delta}\cdot\mathbf{k}\tau_x\sigma_z, \tag{4}$$

which is symmetric under $C_2 = -i\tau_z\sigma_z$, $T = i\sigma_y K$, and $P = \tau_y\sigma_y K$ where $\tau_{x,y,z}$ are the Pauli matrices for particle-hole indices. Gap does not open at zero energy, and an MFL appears along $|\mathbf{k}| = \sqrt{\mu^2 + (\mathbf{\Delta}_0\cdot\mathbf{k})^2}$ [Fig. 3(a)]. The MFL does not disappear by tuning μ and Δ_0, and, in fact, by any continuous deformations preserving the bulk gap. Therefore, a single MFL of this type can appear as the characteristic surface state of odd-C_2 TSCs.

The stability of the above MFL is due to its two $\mathbb{Z}_2$ charges. If we choose a basis in which $S = \mathrm{diag}[1_{N\times N}, -1_{N\times N}]$ and $C_2T = K$,

$$H_{\mathrm{BdG}}(\mathbf{k}) = \begin{pmatrix} 0 & O(\mathbf{k}) \\ O^\dagger(\mathbf{k}) & 0 \end{pmatrix}, \tag{5}$$

where $O(\mathbf{k})$ is real-valued. The 0D topological charge is defined by the sign change of $\det O(\mathbf{k})$ across the MFL, while the 1D topological charge is defined by the winding number of the matrix $O(\mathbf{k})$ around a loop surrounding the MFL [14, 23]

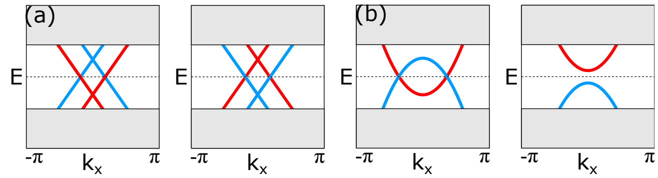

FIG. 3. Single Majorana Fermi line on a C_2-invariant surface of superconductors with odd-C_2 pairing. Shaded regions indicate the bulk energy spectrum of the BdG Hamiltonian. Red and blue lines originate from the electron and hole surface bands, respectively. The spectrum is shown along the k_x direction, but the spectrum looks similar along the k_y direction. (a) Surface band structure near a DCMFL. (b) Surface band structure a MFL with trivial 1D charge. Different stabilities of MFLs in (a) and (b) can be understood from the stability of the parent normal-state Fermi surfaces corresponding to the red line.

Since $O(\mathbf{k}) \xrightarrow{\Delta\to 0} h(\mathbf{k})$, the topological stability of an MFL is inherited from the topological property of the normal-state Fermi surface. The nontrivial 0D charge guarantees that a small perturbation does not gap the Fermi surface and is common to all Fermi surfaces (thus to all MFLs). On the other hand, only the MFL arising from the Fermi surface of a single Dirac fermion carries a nontrivial 1D topological charge (inherited from the π Berry phase of a Dirac fermion) and is robust against any continuous deformations [Fig 3].

Since a DCMFL is realized by odd-$C_{n=2,6}$ pairing, it accompanies gapless hinge states between side surfaces, as shown in the middle panel of Fig. 1(b,d). These hinge states can be understood in terms of the p-wavelike (for odd-C_2 pairing) or f-wavelike (for odd-C_6 pairing) symmetry of the pairing function in real space: when the pairing function changes sign on the side surfaces, gapless hinge states appear as domain wall states [16].

Quartet of Majorana fermions (QMF).— We again consider the surface Dirac fermions of TIs, but with an odd-C_4 pairing function. As $(C_2T)^2 = 1$ and $(C_2P)^2 = -1$, nodes now appear as points at generic momenta [14]. There are two possible C_4 representations for odd-C_4 pairing: $C_{4z} = i\tau_x\sigma_z e^{-i\frac{\pi}{4}\sigma_z}$ and $C_{4z} = \tau_z e^{-i\frac{\pi}{4}\sigma_z}$. In both cases, the pairing term has the form

$$\delta H_\Delta = \Delta_1(\mathbf{k})\tau_x + \Delta_2(\mathbf{k})\tau_x\sigma_x + \Delta_3(\mathbf{k})\tau_x\sigma_y, \tag{6}$$

where the $\Delta_1\tau_x$ term is a potential mass term that anticommutes with the Dirac Hamiltonian $\tau_z\otimes h_D$. The representation $C_{4z} = i\tau_x\sigma_z e^{-i\frac{\pi}{4}\sigma_z}$ allows a mass term $\Delta_1 = m$, thus giving trivial surface states. On the other hand, $C_{4z} = \tau_z e^{-i\frac{\pi}{4}\sigma_z}$ forbids such a constant mass term. In this case, pairing terms split the fourfold degeneracy at $\mathbf{k} = \mathbf{0}$ into four MFs with twofold degeneracy, as shown in Fig. 1(c).

In contrast to HSMFs and DCMFLs, P and S symmetries do not play a critical role in the protection of the QMF, so the surface structure is similar to that in TIs with C_n symmetry [15]. While the presence of S symmetry promotes the $\mathbb{Z}_2$-valued Berry phase of each twofold degenerate MF to the integer-valued winding number, the stability of the MFs as a whole still has a $\mathbb{Z}_2$ character [16]. In the case of odd-C_4 pairing, as the winding numbers of MFs related by C_4 symmetry have opposite signs [16], the total winding number of all MFs is zero. However, MFs carry another $\mathbb{Z}_2$ topological charge instead, indicating their stability when they merge at a C_4-invariant momentum [15, 16]. A QMF is robust because this $\mathbb{Z}_2$ charge is nontrivial.

Similar to the case of DCMFL, the QMF accompanies gapless hinge states between gapped side surfaces, as shown in Fig. 1(c). The appearance of hinge states can be attributed to the d-wavelike symmetry of the pairing function in real space [16].

Lattice model.— To demonstrate our theory, we consider the following model Hamiltonian describing a doped $\mathbb{Z}_2$ TI or Dirac semimetal,

$$\begin{aligned} h_1 = &-\mu + (4 - 2\cos k_x - 2\cos k_y - \cos k_z)\rho_z + \sin k_x \rho_x \sigma_z \\ &- \sin k_y \rho_y + (3\sin k_z(\cos k_y - \cos k_x) + m_0 \sin k_z)\rho_x\sigma_x \\ &+ (-\sin k_z \sin k_x \sin k_y + m_1 \sin k_z)\rho_x\sigma_y, \end{aligned} \quad (7)$$

where $\rho_{i=x,y,z}$ and $\sigma_{i=x,y,z}$ are Pauli matrices for orbital and spin degrees of freedom, respectively. This is symmetric under time reversal $\mathcal{T} = i\sigma_y K$ and mirror operations $\mathcal{M}_x = i\sigma_x$, $\mathcal{M}_y = i\rho_z\sigma_y$, and $\mathcal{M}_z = i\sigma_z$. This model describes a C_{4z} symmetric Dirac semimetal when $m_0 = m_1 = 0$. Nonzero m_0 and m_1, which breaks C_{4z}, M_x and M_y symmetries, opens a gap at bulk Dirac points leading to a $\mathbb{Z}_2$ TI [24, 25].

We first consider even-C_{2z} pairing. When μ is small, as the $\mathbf{k} = (0, 0, k_z)$ line is the only C_2-invariant line crossing the Fermi surface, we need a 1D TSC with $w_+ = -w_- = 2$ along the $\mathbf{k} = (0, 0, k_z)$ line to observe a HSMF on the boundary. If we choose a pairing function $\Delta(\mathbf{k}) = \Delta_e \sin k_z \sigma_z$, the resulting BdG Hamiltonian along the $\mathbf{k} = (0, 0, k_z)$ line is $H_{\rm BdG} = -\mu\tau_z - \cos k_z \rho_z \tau_z + \Delta_e \sin k_z \sigma_z \tau_x$, where $\tau_{i=x,y,z}$ are Pauli matrices for particle-hole indices, and $m_0 = m_1 = 0$ is assumed for simplicity. From this 1D Hamiltonian, we obtain $w_+ = -w_- = 2$ for $C_{2z} = -i\rho_z\sigma_z$ [16]. The associated surface spectrum with a spin-3/2 fermion at $(k_x, k_y) = (0, 0)$ on the C_{2z}-invariant surface is shown in Fig. 4(a). When other even-C_2 pairing terms dominate, nodal or topologically trivial superconductors can also be obtained [16].

On the other hand, in the case of odd-C_2 pairing, as the presence of a single Dirac fermion on the surface is key for observing a DCMFL, any odd-C_2 pairing can induce a DCMFL, thus realizing a C_2-protected TSC as long as the bulk gap fully opens. The surface spectrum for $\Delta(\mathbf{k}) = \Delta_o \rho_x$ is shown in Fig. 4(b). Here, we need both m_0 and m_1 to be nonzero to obtain a fully gapped TSC; otherwise, bulk Dirac points protected by either C_4 symmetry [24, 25] or mirror symmetry [26] appear. In addition to DCMFLs, we obtain helical Majorana hinge states on side surfaces [Fig. 4(c)].

To describe an odd-C_4 TSC with QMF, we need a model whose Fermi surface does not cross C_4-invariant lines; otherwise, the bulk gap does not fully open for odd-C_4 pairing. Hence, instead of Eq. (7), we consider the following model

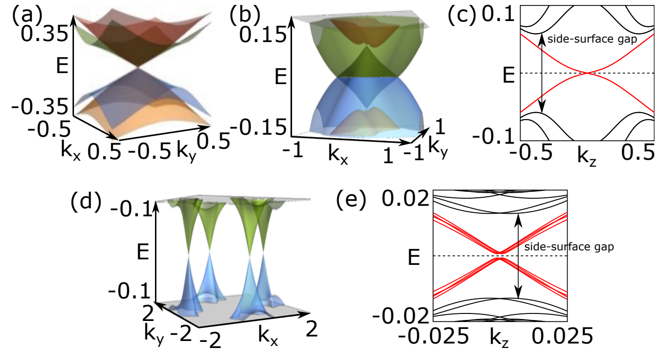

FIG. 4. Boundary Majorana surface states in lattice models. (a) Spin-3/2 MF obtained from Eq. (7) with $\mu = 0.5$, $m_0 = m_1 = 0$ and even-C_2 pairing $\Delta_e = 0.5$. (b) A DCMFL on a C_2 invariant surface obtained from Eq. (7) with $\mu = 0.5$, $m_0 = m_1 = 0.3$ and odd-C_2 pairing $\Delta_o = 0.3$. (c) The helical hinge state (red color) for odd-C_2 pairing obtained from the same Hamiltonian used in (b). (d) A quartet of spin-1/2 MFs obtained from Eq. (8) with $\mu = 0.2$, $M = 1.5$, $\lambda_{\rm SO} = 0.1$, $\Delta_{x^2-y^2} = \Delta_{xy} = 0.5$, and $\Delta_\delta = 0.1$. Associated hinge states (red color) are shown in (e). The splitting of the four C_{4z}-related hinge spectra and small gap at zero energy are finite-size effects, which decrease exponentially as the size of the system grows. The energy spectra in (a), (b), and (d) are calculated with 40 unit cells along the z direction and periodic boundary conditions along the x, y directions. (c) and (e) are calculated with 20×20 unit cells along the x and y directions, and periodic boundary conditions along the z direction.

Hamiltonian for a doped $\mathbb{Z}_2$ TI,

$$\begin{aligned} h_2 = &-\mu + \sin k_z \rho_y + (M - \sum_{i=x,y,z} \cos k_i)\rho_z \\ &+ \lambda_{\rm SO}(\sin k_x \rho_x \sigma_y - \sin k_y \rho_x \sigma_x), \end{aligned} \quad (8)$$

where $\lambda_{\rm SO}$ indicates spin-orbit coupling. h_2 is symmetric under $\mathcal{T} = i\sigma_y K$, $\mathcal{M}_x = i\sigma_x$, $\mathcal{M}_y = i\sigma_y$, $\mathcal{M}_z = i\rho_z\sigma_z$, and $\mathcal{C}_{4z} = e^{-i\frac{\pi}{4}\sigma_z}$. If we take $|\mu|$ larger than the gap induced by $\lambda_{\rm SO}$, the system has a torus-shaped Fermi surface, which is a characteristic of nodal line semimetals. As this Fermi surface does not cross a C_{4z}-invariant line, a fully gapped TSC can be obtained by introducing an odd-C_{4z} pairing. If we consider $\Delta_d(\mathbf{k}) = \Delta_{x^2-y^2}(\cos k_y - \cos k_x)\rho_y\sigma_z + \Delta_{xy}\sin k_x \sin k_y \rho_x + \Delta_\delta(\sin k_x \rho_x \sigma_y + \sin k_y \rho_x \sigma_x)$, the bulk and side-surface gap fully opens and QMF (hinge states) appears on the top surface (side hinges) [Fig. 4(d,e)].

Discussion.— Our model study shows that doped Z_2 TIs having a band structure of massive Dirac semimetals are promising candidates for rotation-protected TSCs. Au_2Pb is such a material [27–29]. It has an orthorhombic symmetry and shows a fully gapped superconductivity below 1.2 K [27]. While this system has been proposed as a TSC, this cannot be a Fu-Kane Z_2 TSC because it does not have Fermi surfaces enclosing a time-reversal-invariant momentum [28, 30–32]. On the other hand, it is more likely that Au_2Pd is a rotation-protected TSC hosting either HSMF or DCMFL. Detailed experimental studies on pairing symmetry and superconducting surface spectrum are desired to test the scenario we propose.

Optical responses may be able to distinguish HSMF and DCMFL because DCMFL can show subgap optical responses down to zero photon energy while other MFs show zero optical response [51]. Finding other characteristic physical responses of unconventional MFs will be a promising future direction.

Interaction and disorder effects on new MFs can be an interesting subject. In the case of HSMFs, the $\mathbb{Z}$ classification will reduce to $\mathbb{Z}_8$, because the winding number in each eigenspace will take a $\mathbb{Z}_8$ value in interacting systems [33–36]. It is an open question whether further modification of the classification will occur. Also, while crystalline-symmetry-protected states are stable against averaged disorder [41–43], the fate of them under strong disorder needs to be studied further.

J.A. thanks SangEun Han and James Jun He for helpful discussions. J.A. was supported by IBS-R009-D1. B.-J.Y. was supported by the Institute for Basic Science in Korea (Grant No. IBS-R009-D1) and Basic Science Research Program through the National Research Foundation of Korea (NRF) (Grant No. 0426-20200003). This work was supported in part by the US Army Research Office under Grant Number W911NF-18-1-0137.

* Present address: Department of Physics, Harvard University, Cambridge, Massachusetts 02138, USA
junyeongahn@fas.harvard.edu
† bjyang@snu.ac.kr

[1] M. Z. Hasan and C. L. Kane, Colloquium: Topological insulators, Rev. Mod. Phys. **82**, 3045 (2010).
[2] B. J. Wieder, B. Bradlyn, Z. Wang, J. Cano, Y. Kim, H.-S. D. Kim, A. M. Rappe, C. L. Kane, and B. A. Bernevig, Wallpaper fermions and the nonsymmorphic Dirac insulator, Science **361**, 246 (2018).
[3] Z. Wang, A. Alexandradinata, R. J. Cava, and B. A. Bernevig, Hourglass fermions, Nature **532**, 189 (2016).
[4] A. Alexandradinata, Z. Wang, and B. A. Bernevig, Topological insulators from group cohomology, Phys. Rev. X **6**, 021008 (2016).
[5] M. P. Kennett, N. Komeilizadeh, K. Kaveh, and P. M. Smith, Birefringent breakup of dirac fermions on a square optical lattice, Phys. Rev. A **83**, 053636 (2011).
[6] B. Bradlyn, J. Cano, Z. Wang, M. Vergniory, C. Felser, R. J. Cava, and B. A. Bernevig, Beyond Dirac and Weyl fermions: Unconventional quasiparticles in conventional crystals, Science **353**, aaf5037 (2016).
[7] L. Liang and Y. Yu, Semimetal with both Rarita-Schwinger-Weyl and Weyl excitations, Phys. Rev. B **93**, 045113 (2016).
[8] P. Tang, Q. Zhou, and S.-C. Zhang, Multiple types of topological fermions in transition metal silicides, Phys. Rev. Lett. **119**, 206402 (2017).
[9] H. Hu, J. Hou, F. Zhang, and C. Zhang, Topological triply degenerate points induced by spin-tensor-momentum couplings, Phys. Rev. Lett. **120**, 240401 (2018).
[10] F. Zhang, C. L. Kane, and E. J. Mele, Time-reversal-invariant topological superconductivity and majorana kramers pairs, Phys. Rev. Lett. **111**, 056402 (2013).
[11] Y. Kim, B. J. Wieder, C. L. Kane, and A. M. Rappe, Dirac line nodes in inversion-symmetric crystals, Phys. Rev. Lett. **115**, 036806 (2015).
[12] C. Fang, Y. Chen, H.-Y. Kee, and L. Fu, Topological nodal line semimetals with and without spin-orbital coupling, Phys. Rev. B **92**, 081201(R) (2015).
[13] D. F. Agterberg, P. M. R. Brydon, and C. Timm, Bogoliubov Fermi surfaces in superconductors with broken time-reversal symmetry, Phys. Rev. Lett. **118**, 127001 (2017).
[14] T. Bzdušek and M. Sigrist, Robust doubly charged nodal lines and nodal surfaces in centrosymmetric systems, Phys. Rev. B **96**, 155105 (2017).
[15] C. Fang and L. Fu, New classes of topological crystalline insulators having surface rotation anomaly, Sci. Adv. **5**, eaat2374 (2019).
[16] See Supplemental Material at [URL will be inserted by publisher] for details on the classification of C_n-symmetric superconductors, spinless models, properties of topological invariants, and the classification of pairing functions in our spin-orbit coupled model systems, which includes [23, 44–50].
[17] K. Shiozaki and M. Sato, Topology of crystalline insulators and superconductors, Phys. Rev. B **90**, 165114 (2014).
[18] E. Cornfeld and A. Chapman, Classification of crystalline topological insulators and superconductors with point group symmetries, Phys. Rev. B **99**, 075105 (2019).
[19] K. Shiozaki, The classification of surface states of topological insulators and superconductors with magnetic point group symmetry, arxiv:1907.09354 (2019).
[20] C. Fang, B. A. Bernevig, and M. J. Gilbert, Topological crystalline superconductors with linearly and projectively represented C_n symmetry, arxiv:1701.01944 (2017).
[21] W. P. Su, J. R. Schrieffer, and A. J. Heeger, Solitons in polyacetylene, Phys. Rev. Lett. **42**, 1698 (1979).
[22] C.-K. Chiu, J. C. Y. Teo, A. P. Schnyder, and S. Ryu, Classification of topological quantum matter with symmetries, Rev. Mod. Phys. **88**, 035005 (2016).
[23] T. Kawakami and M. Sato, Topological crystalline superconductivity in dirac semimetal phase of iron-based superconductors, Phys. Rev. B **100**, 094520 (2019).
[24] S. Kobayashi and M. Sato, Topological superconductivity in dirac semimetals, Phys. Rev. Lett. **115**, 187001 (2015).
[25] T. Hashimoto, S. Kobayashi, Y. Tanaka, and M. Sato, Superconductivity in doped dirac semimetals, Phys. Rev. B **94**, 014510 (2016).
[26] S. A. Yang, H. Pan, and F. Zhang, Dirac and weyl superconductors in three dimensions, Phys. Rev. Lett. **113**, 046401 (2014).
[27] L. M. Schoop, L. S. Xie, R. Chen, Q. D. Gibson, S. H. Lapidus, I. Kimchi, M. Hirschberger, N. Haldolaarachchige, M. N. Ali, C. A. Belvin, *et al.*, Dirac metal to topological metal transition at a structural phase change in Au_2Pb and prediction of Z_2 topology for the superconductor, Phys. Rev. B **91**, 214517 (2015).
[28] Y. Xing, H. Wang, C.-K. Li, X. Zhang, J. Liu, Y. Zhang, J. Luo, Z. Wang, Y. Wang, L. Ling, *et al.*, Superconductivity in topologically nontrivial material Au_2Pb, npj Quantum Materials **1**, 16005 (2016).
[29] Y. Wu, G. Drachuck, L.-L. Wang, D. D. Johnson, P. Swatek, B. Schrunk, D. Mou, L. Huang, S. L. Bud'ko, P. C. Canfield, *et al.*, Electronic structure of the topological superconductor candidate Au_2Pb, Phys. Rev. B **98**, 161107(R) (2018).
[30] L. Fu and E. Berg, Odd-parity topological superconductors: theory and application to $Cu_xBi_2Se_3$, Phys. Rev. Lett. **105**, 097001 (2010).
[31] M. Sato, Topological properties of spin-triplet superconductors and fermi surface topology in the normal state, Phys. Rev. B **79**,

214526 (2009).
[32] M. Sato, Topological odd-parity superconductors, Phys. Rev. B **81**, 220504(R) (2010).
[33] L. Fidkowski and A. Kitaev, Effects of interactions on the topological classification of free fermion systems, Phys. Rev. B **81**, 134509 (2010).
[34] L. Fidkowski and A. Kitaev, Topological phases of fermions in one dimension, Phys. Rev. B **83**, 075103 (2011).
[35] A. M. Turner, F. Pollmann, and E. Berg, Topological phases of one-dimensional fermions: An entanglement point of view, Phys. Rev. B **83**, 075102 (2011).
[36] Y.-Z. You, Z. Wang, J. Oon, and C. Xu, Topological number and fermion green's function for strongly interacting topological superconductors, Phys. Rev. B **90**, 060502(R) (2014).
[37] T. Grover, D. Sheng, and A. Vishwanath, Emergent space-time supersymmetry at the boundary of a topological phase, Science **344**, 280 (2014).
[38] P. Ponte and S.-S. Lee, Emergence of supersymmetry on the surface of three-dimensional topological insulators, New Journal of Physics **16**, 013044 (2014).
[39] T. H. Hsieh, G. B. Halász, and T. Grover, All majorana models with translation symmetry are supersymmetric, Phys. Rev. Lett. **117**, 166802 (2016).
[40] S. Han, J. Lee, and E.-G. Moon, Lattice vibration as a knob for novel quantum criticality: Emergence of supersymmetry from spin-lattice coupling, arXiv preprint arXiv:1911.01435 (2019).
[41] L. Fu and C. L. Kane, Topology, delocalization via average symmetry and the symplectic anderson transition, Physical review letters **109**, 246605 (2012).
[42] T. H. Hsieh, H. Lin, J. Liu, W. Duan, A. Bansil, and L. Fu, Topological crystalline insulators in the SnTe material class, Nat. Commun. **3**, 982 (2012).
[43] C. Fang and L. Fu, New classes of three-dimensional topological crystalline insulators: Nonsymmorphic and magnetic, Phys. Rev. B **91**, 161105(R) (2015).
[44] A. P. Schnyder, S. Ryu, A. Furusaki, and A. W. W. Ludwig, Classification of topological insulators and superconductors in three spatial dimensions, Phys. Rev. B **78**, 195125 (2008).
[45] J. Ahn, D. Kim, Y. Kim, and B.-J. Yang, Band topology and linking structure of nodal line semimetals with Z_2 monopole charges, Phys. Rev. Lett. **121**, 106403 (2018).
[46] E. Khalaf, Higher-order topological insulators and superconductors protected by inversion symmetry, Phys. Rev. B **97**, 205136 (2018).
[47] M. Geier, L. Trifunovic, M. Hoskam, and P. W. Brouwer, Second-order topological insulators and superconductors with an order-two crystalline symmetry, Phys. Rev. B **97**, 205135 (2018).
[48] Y. Hwang, J. Ahn, and B.-J. Yang, Fragile topology protected by inversion symmetry: Diagnosis, bulk-boundary correspondence, and wilson loop, Phys. Rev. B **100**, 205126 (2019).
[49] B. Bradlyn, Z. Wang, J. Cano, and B. A. Bernevig, Disconnected elementary band representations, fragile topology, and wilson loops as topological indices: An example on the triangular lattice, Phys. Rev. B **99**, 045140 (2019).
[50] A. Bouhon, A. M. Black-Schaffer, and R.-J. Slager, Wilson loop approach to fragile topology of split elementary band representations and topological crystalline insulators with time-reversal symmetry, Phys. Rev. B **100**, 195135 (2019).
[51] J. Ahn and N. Nagaosa, Theory of optical responses in clean multiband superconductors, Nat. Commun. **12**, 1617 (2021).